Cell Reports Medicine, Volume *4*

Supplemental information

Tissue-resident memory CAR T cells with stem-like characteristics display enhanced efficacy against solid and liquid tumors

In-Young Jung, Estela Noguera-Ortega, Robert Bartoszek, Sierra M. Collins, Erik Williams, Megan Davis, Julie K. Jadlowsky, Gabriela Plesa, Donald L. Siegel, Anne Chew, Bruce L. Levine, Shelley L. Berger, Edmund K. Moon, Steven M. Albelda, and Joseph A. Fraietta

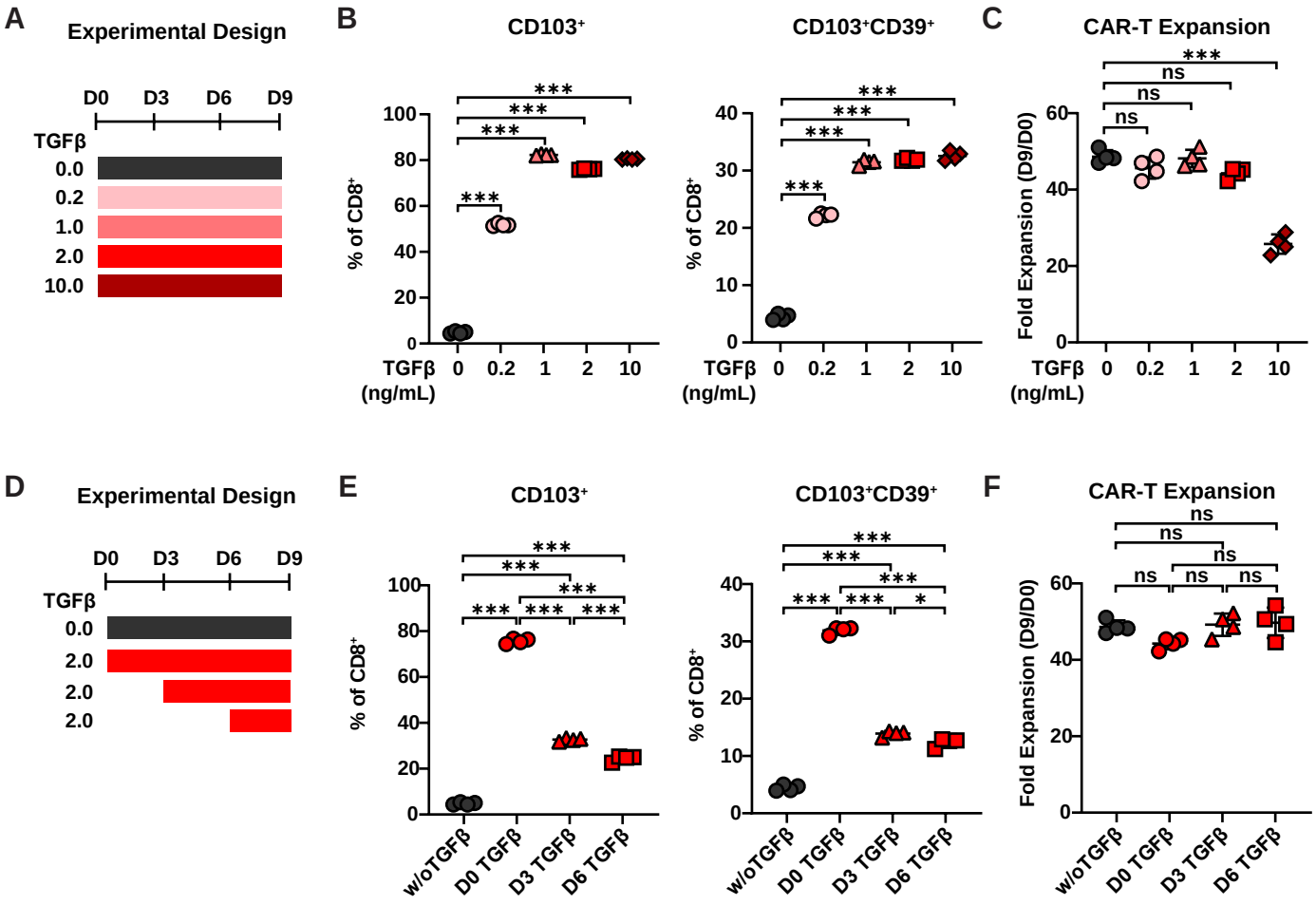
A
Experimental Design
D0
D3
D6
D9
TGFβ
0.0
0.2
1.0
2.0
10.0
B
CD103+
CD103+CD39+
% of CD8+
TGFβ (ng/mL)
0
0.2
1
2
10
***
C
CAR-T Expansion
Fold Expansion (D9/D0)
ns
D
Experimental Design
2.0
2.0
2.0
E
CD103+
CD103+CD39+
w/oTGFβ
D0 TGFβ
D3 TGFβ
D6 TGFβ
*
F
CAR-T Expansion

Supplementary Figure 1. Optimization of CAR-T_{RM} culture conditions. Related to Figure 1. (**A**) Schematic of optimizing TGF-β concentration. (**B**) Frequencies of $CD103^+$ and $CD103^+CD39^+$ $CD8^+$ CAR T-cells with 0, 0.2, 1, 2, 10 ng/mL TGF-β added during CAR T-cell manufacturing. (**C**) Fold CAR T-cell expansion during manufacturing with TGF-β concentration as indicated in panel **A**. (**D**) Schematic of optimizing duration of TGF-β exposure. (**E**) Frequencies of $CD103^+$ and $CD103^+CD39^+$ $CD8^+$ CAR T-cells with TGF-β added at different timepoints during CAR T-cell manufacturing. (**F**) Fold CAR T-cell expansion during manufacturing with TGF-β added on different timepoints as indicated in panel **D**. One-way ANOVA, $n = 4$ biological replicates. $*P < 0.05$, $*P < 0.01$, $***P < 0.001$, ns.: not significant.

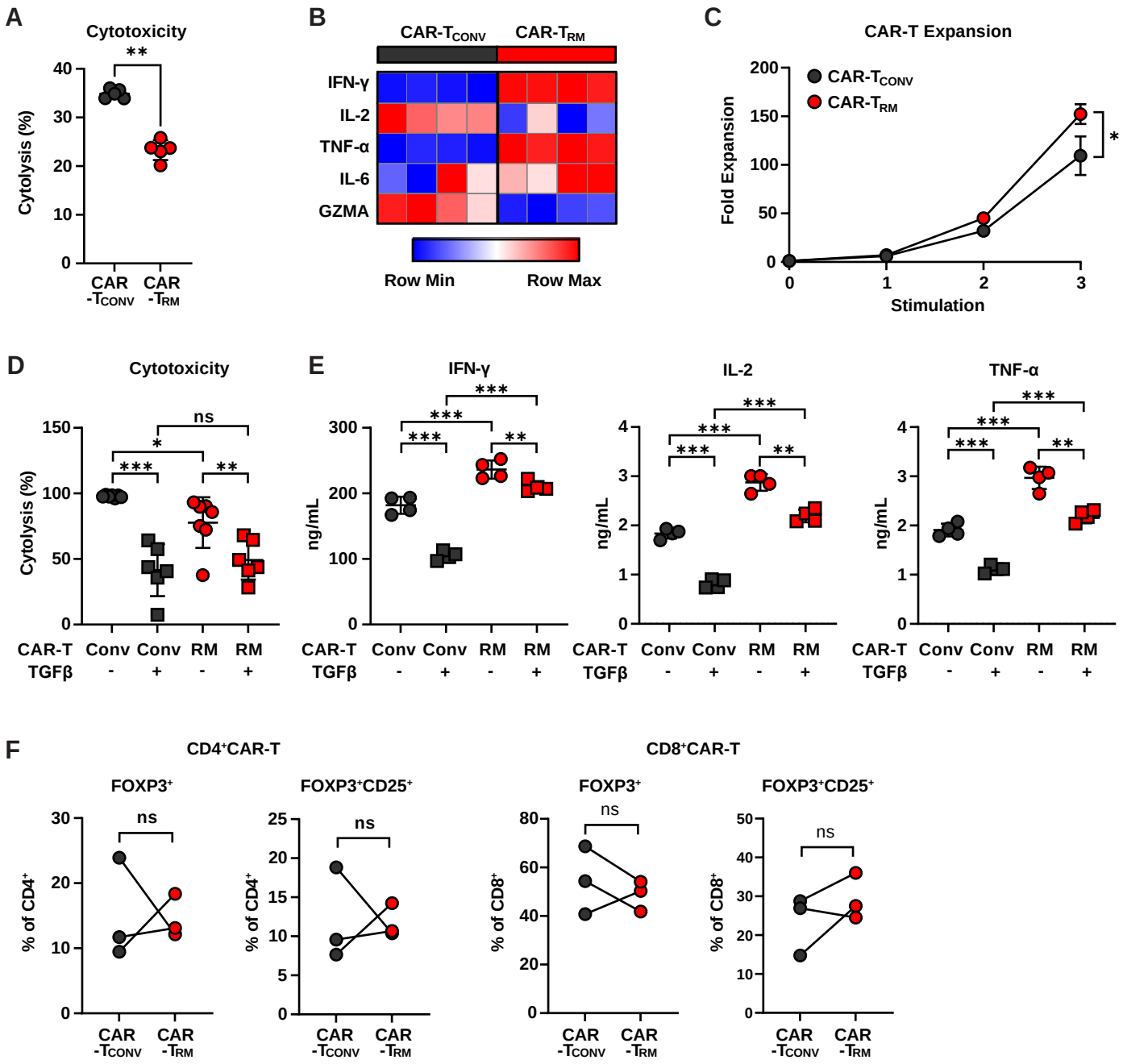
A
Cytotoxicity
Cytolysis (%)
CAR -TCONV
CAR -TRM
B
CAR-TCONV
CAR-TRM
IFN-γ
IL-2
TNF-α
IL-6
GZMA
Row Min
Row Max
C
CAR-T Expansion
CAR-TCONV
CAR-TRM
Fold Expansion
Stimulation
D
Cytotoxicity
Cytolysis (%)
CAR-T
TGFβ
Conv Conv RM RM
E
IFN-γ
IL-2
TNF-α
ng/mL
F
CD4+CAR-T
CD8+CAR-T
FOXP3+
FOXP3+CD25+
% of CD4+
% of CD8+
ns

Supplementary Figure 2. Characterization of CAR-T_{RM} cells. Related to Figure 1.

(**A**) M5 CAR T-cells were isolated after three consecutive tumor challenges and co-cultured with Capan-2 target cells at an effector to target ratio of 1:2. Cytotoxic capacity at 7-hours post- co-culture is shown (Mann-Whitney test, $n = 5$ biological replicates). (**B**) Cytokine production after a second challenge with AsPC1 tumor cells. (**C**) Fold CAR T-cell expansion during a restimulation assay (Mann-Whitney test, $n = 4$ biological replicates). Experiments in panels **B-C** were conducted using CAR T-cells manufactured from different healthy donors. Figures display representative results from one donor. (**D, E**) M5 CAR T-cells were incubated with Capan-2 target cells at an effector to target ratio of 1:3 in presence or absence of 2 ng/mL TGFβ. The experiments were performed using CAR T-cells generated from individual healthy donors/biological replicates. (**D**) Cytolytic activity of CAR T-cells 4-days post-coculture. (**E**) Effector cytokine production 24-hours after co-incubation (one-way ANOVA, $n = 4$ biological replicates). (**F**) Frequencies of $FOXP3^+$ and $FOXP3^+CD25^+$ CAR T-cells after manufacturing (paired *t*-test, $n = 3$ biological replicates). $*P < 0.05$, $*P < 0.01$, $***P < 0.001$, ns.: not significant.

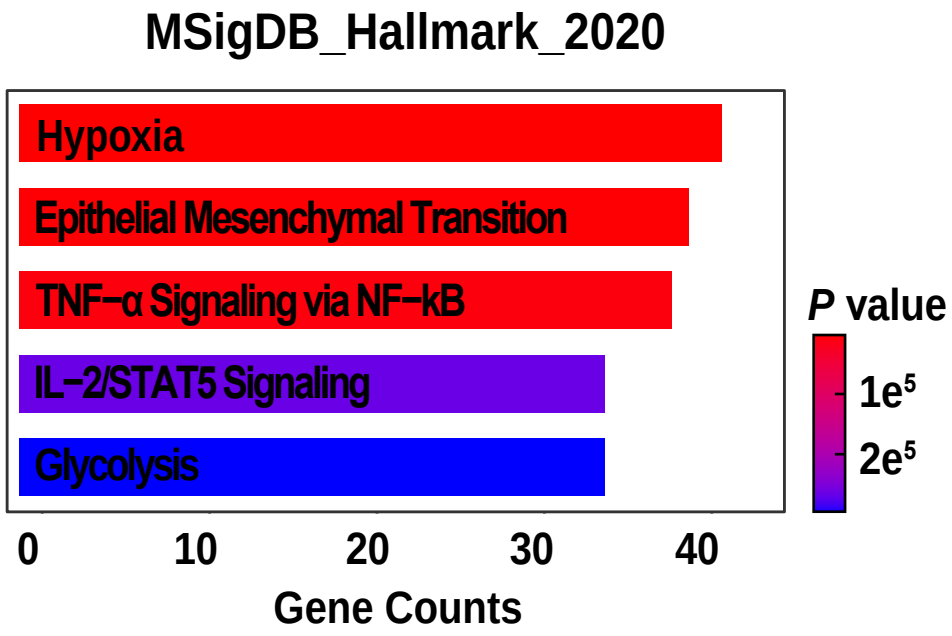
MSigDB_Hallmark_2020
Hypoxia
Epithelial Mesenchymal Transition
TNF−α Signaling via NF−kB
IL−2/STAT5 Signaling
Glycolysis
0
10
20
30
40
Gene Counts
P value
1e5
2e5

Supplementary Figure 3. Top pathways enriched in CAR-T_{RM} cells. Related to Figure 2.

Pathway analysis using Enrichr was carried out with genes upregulated in $CD8^+$ CAR-T_{RM} cells compared to $CD8^+$CAR-T_{CONV} cells (MSigDB_Hallmark_2020).

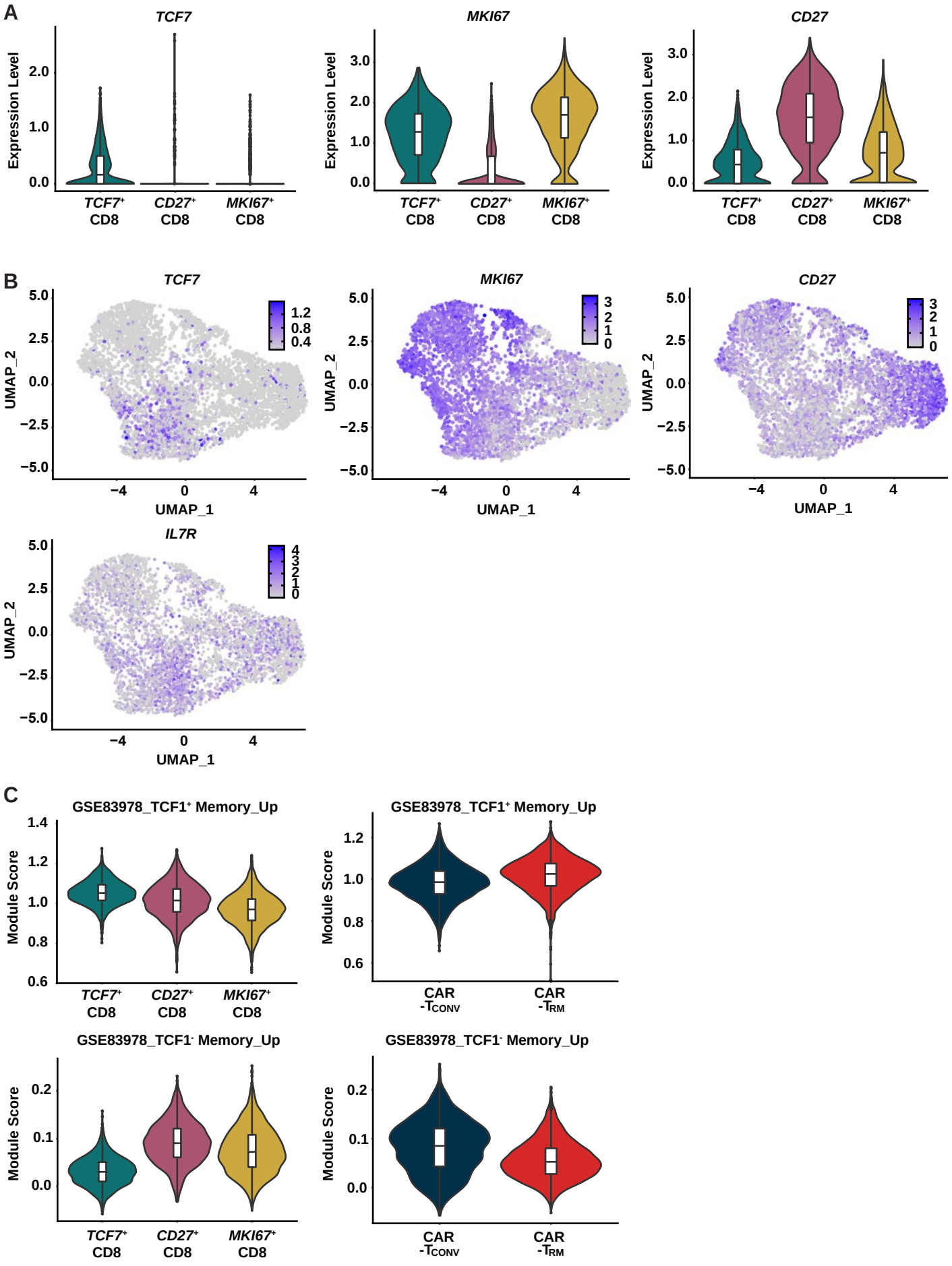
A
TCF7
MKI67
CD27
Expression Level
TCF7+ CD8
CD27+ CD8
MKI67+ CD8
B
TCF7
MKI67
CD27
IL7R
UMAP_1
UMAP_2
C
GSE83978_TCF1+ Memory_Up
GSE83978_TCF1- Memory_Up
Module Score
CAR -TCONV
CAR -TRM

Supplementary Figure 4. Single-cell gene expression analysis of CAR-T_{CONV} and CAR-T_{RM} cells. Related to Figure 3. (**A**) Violin plots displaying expression of cluster-defining markers in $CD8^+$ CAR T-cells. (**B**) UMAP plots illustrating expression levels of the same markers in the $CD8^+$ CAR T-cell population. (**C**) Module scores for 'stem-like' ($TCF1^+$ memory $CD8^+$ T-cells) and 'non-stem-like' ($TCF1^-$ memory $CD8^+$ T-cells) T-cell signatures were calculated for CD8 clusters and CAR T-cell samples (GSE83978).

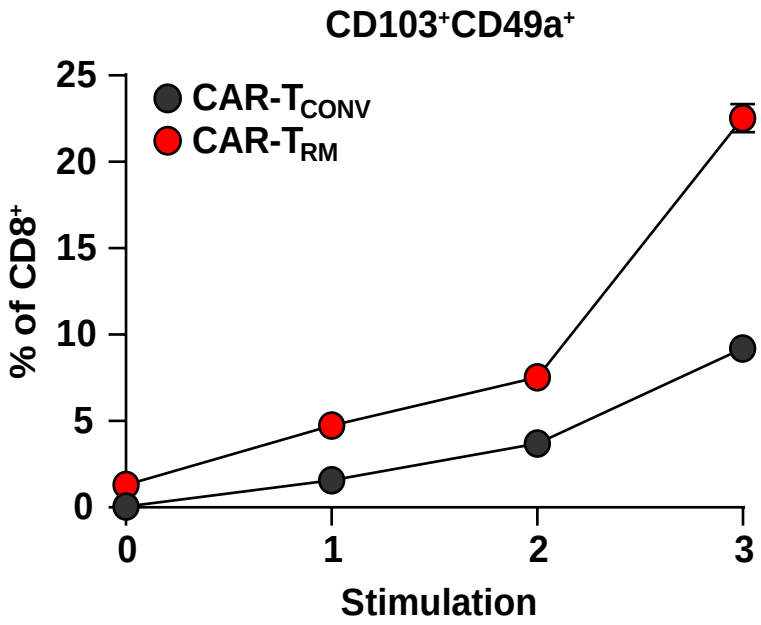
CD103+CD49a+
CAR-TCONV
CAR-TRM
% of CD8+
25
20
15
10
5
0
0
1
2
3
Stimulation

Supplementary Figure 5. Sustained resident memory phenotype of CAR-T_{RM} cells during chronic antigen stimulation. Related to Figure 4. Anti-mesothelin CAR T-cells were serially challenged with AsPC1 tumor cells, and frequencies of resident memory ($CD103^+CD49a^+CD8^+$) T-cells were assessed over time.

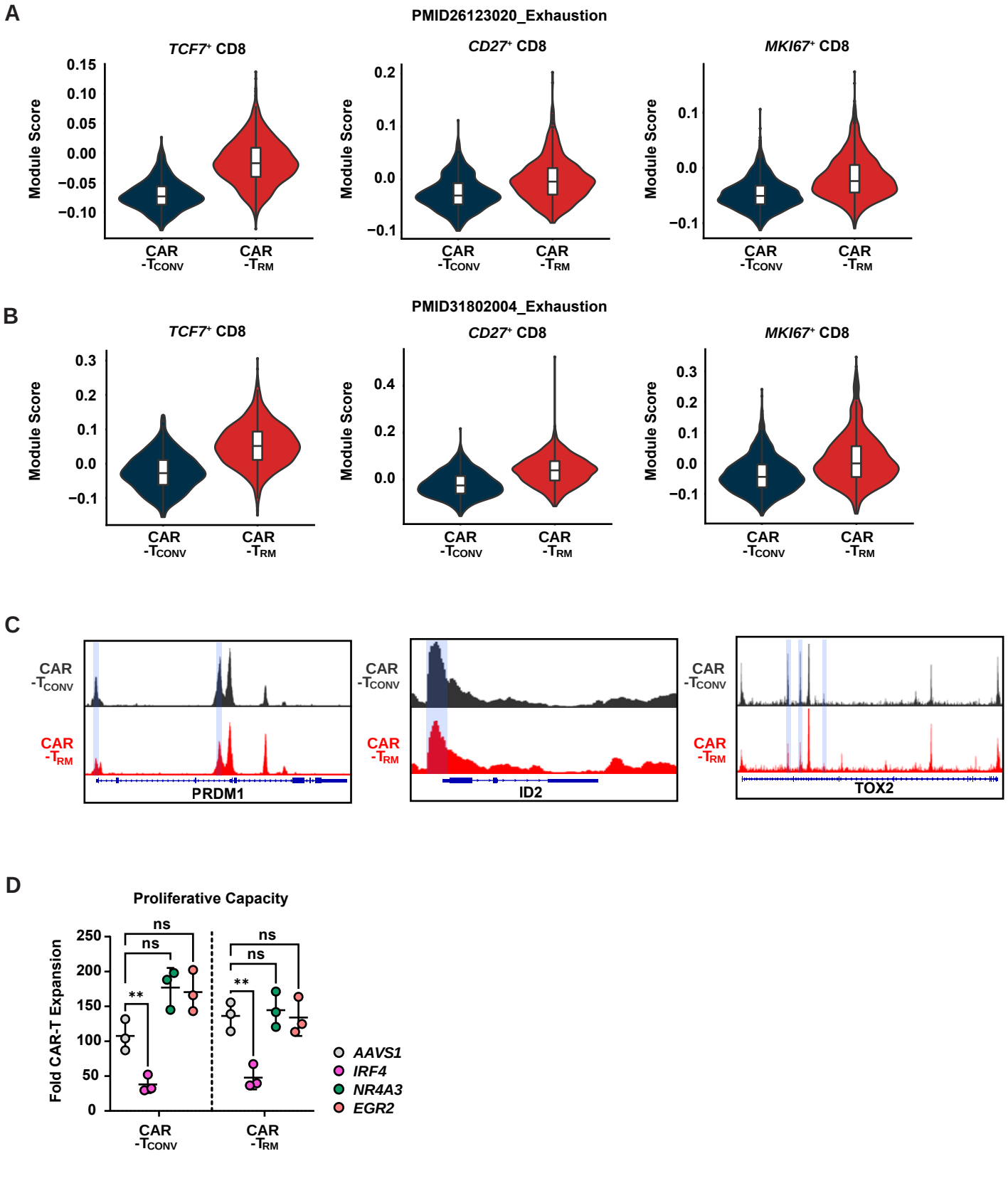
A
PMID26123020_Exhaustion
TCF7+ CD8
CD27+ CD8
MKI67+ CD8
Module Score
CAR -TCONV
CAR -TRM
B
PMID31802004_Exhaustion
C
PRDM1
ID2
TOX2
D
Proliferative Capacity
Fold CAR-T Expansion
ns
**
AAVS1
IRF4
NR4A3
EGR2

Supplementary Figure 6. Exhaustion features in CAR-T_{RM} cells. Related to Figure 5.

(**A, B**) Exhaustion scores are compared between CAR-T_{CONV} and CAR-T_{RM} in each $CD8^+$ T-cell cluster. (**A**) PMID26123020 (**B**) PMID31802004. (**C**) ATAC-seq tracks of *PRDM1*, *ID2*, and *TOX2*. Differentially accessible regions are highlighted in blue. (**D**) M5 CAR T-cells were serially challenged with AsPC1 cells at an E:T ratio of 2:1. Fold CAR T-cell expansion after the third round of antigen stimulation is shown (two-way ANOVA, $n = 3$ biological replicates). $^*P < 0.05$, $^*P < 0.01$, $^{***}P < 0.001$, ns.: not significant.

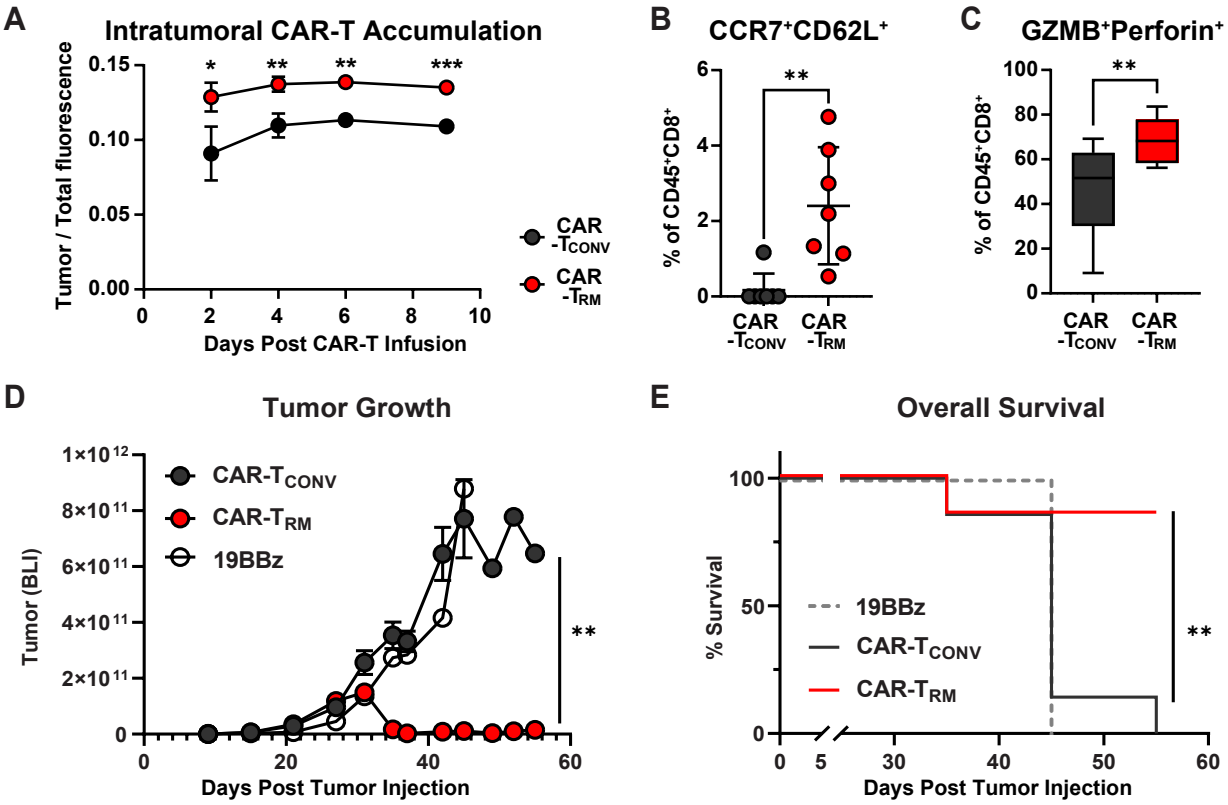
A
Intratumoral CAR-T Accumulation
Tumor / Total fluorescence
0.15
0.10
0.05
0.00
0
2
4
6
8
10
Days Post CAR-T Infusion
*
**
**
***
CAR -TCONV
CAR -TRM
B
CCR7+CD62L+
% of CD45+CD8+
6
4
2
0
**
CAR -TCONV
CAR -TRM
C
GZMB+Perforin+
% of CD45+CD8+
100
80
60
40
20
0
**
CAR -TCONV
CAR -TRM
D
Tumor Growth
Tumor (BLI)
1×10 12
8×10 11
6×10 11
4×10 11
2×10 11
0
0
20
40
60
Days Post Tumor Injection
CAR-TCONV
CAR-TRM
19BBz
**
E
Overall Survival
% Survival
100
50
0
0
5
30
40
50
60
Days Post Tumor Injection
19BBz
CAR-TCONV
CAR-TRM
**

Supplementary Figure 7. CAR-T_{RM} cell immunophenotype and antitumor efficacy in pancreatic and prostate cancer models. Related to Figure 6. (**A-C**) Capan-2 pancreatic cancer xenograft model: (**A**) NSG mice engrafted with 4×10^6 Capan-2 cells received M5 CAR-T_{CONV} and CAR-T_{RM} cells labeled with near-infrared (NIR) fluorescent dye intravenously on day 33 post-engraftment. NIR intensity was monitored over time (Unpaired *t*-test, $n = 3$ biological replicates). (**B**) Frequencies of $hCD45^+CD8^+$ cells in tumors expressing CCR7 and CD62L are shown (Mann-Whitney test, $n = 7$ biological replicates). (**C**) Tumor-infiltrating CAR T-cells were reactivated with phorbol 12-myristate 13-acetate and ionomycin, followed by measurement of effector molecule elaboration (Mann-Whitney test, $n = 12$ biological replicates). (**D-E**) Intraosseous PC3-PSMA prostate tumor model: (**D**) Male NSG mice intrafemorally engrafted with 2×10^5 PC3-PSMA cells received 1×10^5 anti-PSMA CAR-T_{CONV} or CAR-T_{RM} cells, or control CD19-targeting CAR T-cells (19BBz) intravenously on day 21 post-implantation ($n = 7$ biological replicates per group). Tumor burden was assessed by bioluminescent imaging after intraperitoneal injection of luciferin and quantification with the Xenogen IVIS Imaging System (one-way ANOVA). (**E**) Kaplan-Meier survival curves show prolonged survival in the CAR-T_{RM} group compared to CAR-T_{CONV} (Log-rank test). $^*P < 0.05$, $^{**}P < 0.01$, $^{***}P < 0.001$, ns: not significant.